Excited States and Reduced and Oxidized Forms of $C_{76}(D_2)$ and $C_{78}(C_{2v}')$

Dirk M. Guldi,*,† Di Liu, and Prashant V. Kamat*,‡

Radiation Laboratory, University of Notre Dame, Notre Dame, Indiana 46556

Received: April 7, 1997; In Final Form: June 27, 1997[⊗]

The singlet and triplet excited state properties of $C_{76}(D_2)$ and $C_{78}(C_{2v}')$ have been investigated using picosecond laser flash photolysis and pulse radiolysis. Both C_{76} and C_{78} are weakly fluorescent as they undergo internal nonradiative conversion and intersystem crossing to generate a triplet excited state. Unlike their predecessor, C_{60}, the excited larger fullerenes have structured spectral bands in the visible/NIR region. The triplet excited states of C_{76} and C_{78} were also generated independently by energy transfer from triplet excited biphenyl with a diffusion-controlled rate ($k_{et} \approx 1 \times 10^{10}$ s^{-1}). These larger fullerenes readily undergo one-electron reduction and oxidation by reacting with radiolytically generated $(CH_3)_2{}^{\bullet}C(OH)$ and $(CH_2Cl_2)^{\bullet+}$ radicals. The absorption features of excited states and chemical reactivity of C_{76} and C_{78} are compared with those of C_{60}, C_{70}, and C_{84}. The characterization of radical anions of these larger fullerenes is also made with complementary reduction experiments with UV-irradiated TiO_2 nanoparticles.

Introduction

The photophysical and redox properties of the most abundant fullerene, namely, C_{60}, have been well-documented, due to its relative ease of isolation and its subsequent macroscopic production. In contrast, the relatively small synthetic amounts of larger fullerenes (C_{76}, C_{78}, C_{84}, etc.) produced during the contact-arc vaporization of graphite restrict their availability for general purposes. The presence of more than a single isomer which satisfies the isolated-pentagon rule results in further complications in separating these isomeric fullerenes. For example, C_{76} is chiral and usually exists in D_2 symmetry, while MO theory predicts five possible isomers for C_{78}.[1] Several of these isomers (C_{2v}, C_{2v}', and chiral D_3) have been isolated, and preliminary characterization has been made using NMR and UV/visible/IR and resonance Raman spectroscopy.[2−9]

In our recent studies we characterized the excited states and radical intermediates of C_{84} using fast kinetic spectroscopy.[10,11] However, the information available until now regarding the physicochemical properties of other larger fullerenes is rather limited. Both C_{76} and C_{78} undergo multistep reversible reductions and an irreversible oxidation.[12,13] The reported reduction potentials for C_{76} and C_{78} are −0.83 and −0.77 V vs the ferrocene couple, Fc/Fc^+, while the oxidation potentials of C_{76} and C_{78} are around 0.81 and 0.95 V vs the Fc/Fc^+ couple. These one-electron reduction and oxidation potentials of higher fullerenes are lower compared to those of C_{60} ($E^\circ_{red} = -1.06$ V and $E^\circ_{ox} = 1.26$ V vs the Fc/Fc^+ couple). Therefore these larger carbon allotropes should be better electron acceptor and donor moieties than C_{60}. These larger fullerenes, namely, C_{76} and C_{78}, can also serve as photosensitizers or electron relays in photoinduced electron transfer reactions. We have now investigated the excited state and redox properties of $C_{76}(D_2)$ and $C_{78}(C_{2v}')$ using laser flash photolysis and pulse radiolysis experiments. Transient absorption measurements that characterize one-electron reduction and oxidation products and the kinetic details of their chemical reactivity are presented here.

Experimental Section

$C_{76}(D_2)$ and $C_{78}(C_{2v}')$ were purchased from Techno Carbo (France). The fullerene samples as monitored by HPLC were at least of 98.93% for $C_{76}(D_2)$ (containing ∼0.44% of a minor isomer) and 99.85% purity for $C_{78}(C_{2v}')$. Absorption spectra were recorded with a Milton Roy Spectronic 3000 Array spectrophotometer.

Laser Flash Photolysis. Picosecond laser flash photolysis experiments were carried out with 532-nm laser pulses from a mode-locked, Q-switched Quantel YG-501 DP ND:YAG laser system (pulse width = 18 ps, 2−3 mJ/pulse). The white continuum picosecond probe pulse was generated by passing the fundamental output through a D_2O/H_2O solution. The probe was fed to a spectrograph (HR-320, ISDA Instruments, Inc.) with fiber optic cables, and was analyzed with a dual diode array detector (Princeton Instruments, Inc.) interfaced with an IBM-AT computer.

Pulse Radiolysis. Pulse radiolysis experiments were performed by utilizing 50-ns pulses of 8-MeV electrons from a Model TB-8/16-1S Electron Linear Accelerator. Dosimetry was based on the oxidation of SCN^- to $(SCN)_2^{\bullet-}$ (G value = 6 in N_2O-saturated aqueous solutions. (The G value denotes the number of species generated per 100 eV, or the approximate micromolar concentration per 10 J of absorbed energy.) The radical concentration generated per pulse amounts to $(1-3) \times 10^{-6}$ M for all the systems investigated in this study.

Results and Discussion

Absorption Characteristics. Efforts have been made recently to characterize the absorption and electrochemical properties of C_{76} and C_{78}.[2,12−14] Their solubility in nonpolar solvents (≥0.1 mM) makes it possible to employ them in conventional as well as transient absorption measurements. The absorption spectra of C_{76} and C_{78} in methylcyclohexane are compared to that of C_{60} in Figure 1. While the solution of C_{60} is magenta colored, the solutions of C_{76} and C_{78} are yellow-green. Like C_{60} and C_{70} both these larger fullerenes absorb strongly in the UV and visible, but the increase in carbon atom count and change in symmetry alter the nature of electronic and vibrational transitions. The absorption in the visible and ease of inducing reversible reduction make these higher fullerenes potentially useful as photosensitizers and/or building blocks for electron relay systems. In order to evaluate their

† GULDI@MARCONI.RAD.ND.EDU.
‡ KAMAT.1@ND.EDU or http://www.nd.edu/∼pkamat.
⊗ Abstract published in *Advance ACS Abstracts,* August 15, 1997.

S1089-5639(97)01190-0 CCC: $14.00

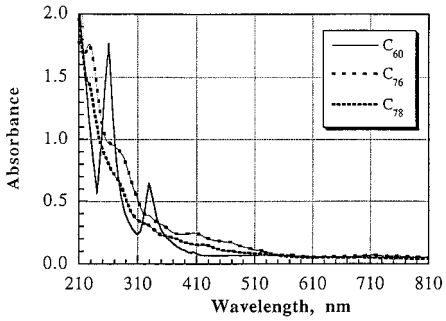

Figure 1. Absorption spectra of C_{76} and C_{78} in methylcyclohexane. The absorption spectrum of C_{60} is shown for comparison.

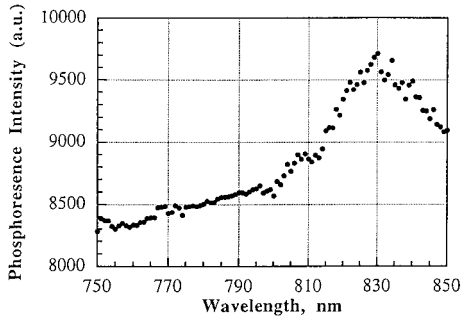

Figure 2. Phosphorescence related emission of C_{78} (5.0×10^{-5} M) in methylcyclohexane, 2-methyltetrahydrofuran, and ethyl iodide (2:1:1 v/v) at 77 K; excitation wavelength 337 nm.

excited state and redox properties, we have now carried out a series of steady state and time-resolved spectroscopy measurements.

Phosphorescence Measurements. Both C_{76} and C_{78} are weakly fluorescent as they undergo efficient intersystem crossing to generate a triplet excited state. This intersystem crossing process can be further accelerated by inducing an external heavy atom effect. For example, the incorporation of ethyl iodide is known to accelerate the rate of intersystem crossing from excited singlet to triplet state. Thus, the fluorescence emission of C_{76} and C_{78} is suppressed in a solvent mixture of methylcyclohexane, 2-methyltetrahydrofuran, and ethyl iodide (2:1:1 v/v), and this enables observation of phosphorescence emission from the triplet excited state.

Figure 2 shows the phosphorescence spectrum of C_{78} at 77 K. A group of four emission lines were observed with maxima at 808, 823, 830, and 840 nm for C_{78} with relative intensities similar to a previous report[15] on C_{60}-related emission. Although less resolved, the presence of broad peaks confirms that the emission originates from the excited triplet state. We assign the weak band at 808 nm to the $T_1 \rightarrow S_0$ ($0 \rightarrow 0$) transition. Similarly the $0 \rightarrow 0$ transition of triplet excited C_{76} to its ground state is seen at 806 nm. It should be noted that these shifts, relative to C_{60} ($E_T(C_{60}) = 36.38$ kcal/mol), are in line with the red-shifted emission of pristine C_{70} and indicate energetically lower lying excited triplet levels for C_{76} and C_{78}. From the $0 \rightarrow 0$ transition we estimate the triplet energies of C_{76} and C_{78} to be 35.4 kcal/mol.

Phosphorescence measurements were also carried out in neat methylcyclohexane by employing a short time delay between the excitation and emission detection. The phosphorescence was rather weak, but the general observations were identical to the ethyl iodide induced phosphorescence data. These measurements provide fundamental information of the fullerene's energy level and the redox potential of their excited states.

Pico- and Nanosecond Flash Photolysis. In order to probe the excited singlet and triplet state characteristics of C_{76} and

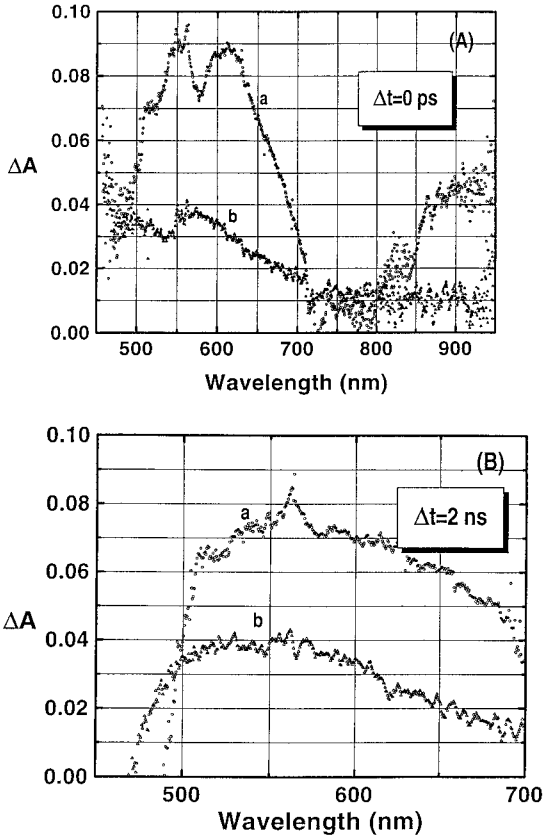

Figure 3. Transient absorbance changes observed following picosecond flash photolysis (A) immediately and (B) 2000 ps after 355-nm laser pulse (pulse width 18 ps, 1.6 mJ) excitation. The difference absorption spectra were recorded following excitation of (a) C_{76} and (b) C_{78} (2.0×10^{-5} M) in deaerated toluene.

C_{78}, time-resolved absorption spectra were recorded following picosecond laser excitation. Figure 3A,B displays the absorption changes recorded following 355-nm laser pulse excitation (pulse width 18 ps) of 2.0×10^{-5} M C_{76} and C_{78} in deaerated toluene solution at $\Delta t = 0$ ps and 2000 ps, respectively. The transient absorption spectrum recorded immediately after the laser pulse corresponds to the singlet excited state. The singlet excited C_{76} is characterized by broad absorption maxima at 560, 620, and 900 nm (see Table 1). On the other hand the excited singlet of C_{78} absorbs weakly in the 450−950 nm region. However, no characteristic absorption maximum could be identified in this case. The decay of the $^1C_{76}$* followed clean first-order kinetics with a lifetime of about 1.25 ns. We also observed a growth of some weak and broad absorption in the 560−640 nm region (Figure 3B), in parallel with the decay of the singlet excited state. This we attribute to the formation of energetically lower lying triplet excited states. The intersystem crossing that leads to the formation of triplet excited states can be described as

$$C_{76} \xrightarrow{h\nu} (^1C_{76}^*) \xrightarrow{ISC} (^3C_{76}^*) \qquad (1)$$

The intersystem crossing is expected to be one of the major deactivation steps for the excited singlet state since fullerenes are weakly fluorescent and exhibit significant amounts of triplet formation.[16] The rate constant for the intersystem crossing process as measured from the decay of the excited singlet state of C_{76} is 8.0×10^8 M^{-1} s^{-1}, which is similar to the one observed for pristine C_{60}.

A complementary technique of nanosecond flash photolysis was also employed to confirm the difference absorption changes

TABLE 1: Photophysical Properties of $C_{76}(D_2)$, $C_{78}(C_{2v}')$, and other Fullerenes

fullerene	singlet−singlet	triplet−triplet	triplet quantum yield	radical cation	radical anion
C_{60} (from refs 18, 21, 35)	920	400, 750	0.93	980	1080
C_{70} (from refs 36, 37)	∼660	435, 970	0.90	930	880
$C_{76}(D_2)$	560, 620, 900	560−640	0.05	960	905
$C_{78}(C_{2v}')$	890	490	0.12	975	975
C_{84} (from ref 19)		310		920	960

TABLE 2: Comparison of Kinetic Properties of $C_{76}(D_2)$ and $C_{78}(C_{2v}')$, with Other Fullerenes

fullerene	$E°_{red}$ (V vs Fc/Fc$^+$) ref 12	$E°_{ox}$ (V vs Fc/Fc$^+$) ref 12	rate constant for T−T energy transfer from ^{3}(BP)* (10^{10} M^{-1} s^{-1})	rate constant for reduction with $(CH_3)_2$•COH (10^9 M^{-1} s^{-1})
C_{60}	−1.06	1.26	1.7	0.85
C_{70}	−1.02	1.20	2.0	0.8
$C_{76}(D_2)$	−0.83	0.81	1.1	1.3
$C_{78}(C_{2v}')$	−0.77	0.95	1.3	1.6
C_{84}	−0.67	0.93	0.4	

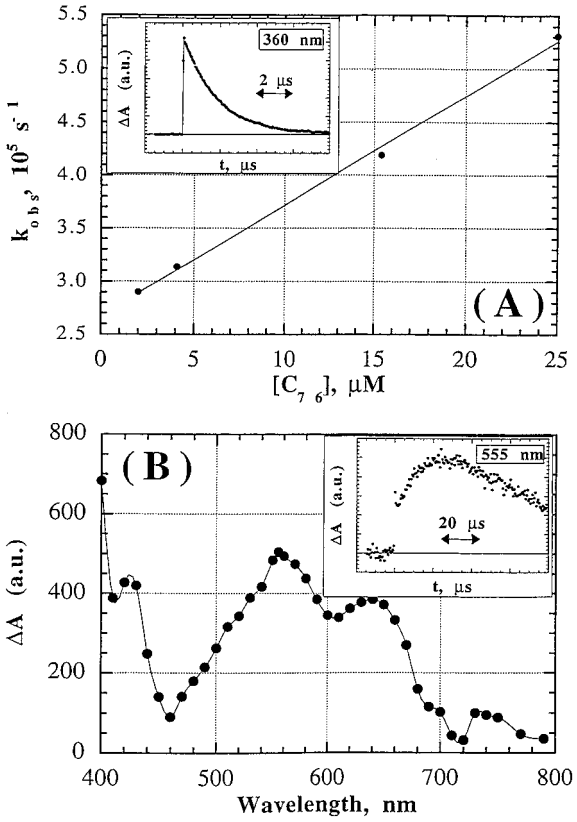

Figure 4. (A) Plot of k_{obs} vs initial concentration of C_{76} representing bimolecular triplet-triplet energy transfer between ^{3}BP* (0.02 M) and ground state C_{76} in deoxygenated toluene. The absorption−time profile recorded at 360 nm recorded in the presence of 1.55×10^{-5} M C_{76} is shown in the inset. (B) Difference absorption spectrum recorded 20 μs after the electron pulse in a nitrogen-saturated toluene solution containing 0.02 M biphenyl and 4.0×10^{-6} M C_{76}. The absorption−time profile recorded at 555 nm shows the formation of $^3C_{76}$ and its decay.

involving the formation of ($^3C_{76}$*). Laser pulse excitation (pulse width 6 ns) at 337 nm of a deaerated methylcyclohexane solution of C_{76} resulted in a transient absorption change, which displays broad maxima at 555 and 650 nm. The absorption band in general resembled the one detected in the picosecond experiments.

Kinetic analysis of both bleaching and formation traces of time−absorption profiles (C_{76} and C_{78}) revealed a recovery of the transient absorption to the original base line in an exponential manner. The excited triplet states of C_{76} and C_{78} decayed with half-lives typically in the range of 3.2 and 3.8 μs, respectively. These values are smaller than the previously reported values for pristine C_{60} in methylcyclohexane or toluene and are influenced by the T−T annihilation and ground state quenching processes.

Triplet Quantum Yield Measurements. Triplet quantum yields of C_{76} and C_{78} were measured using the triplet−triplet energy transfer method. The triplet excited state fullerene was the donor species, and a crown ether functionalized squaraine dye was the acceptor species. Details of T−T energy transfer between $^3C_{60}$* and squaraine dye have been presented in our earlier studies.[17] The intensity of 337-nm laser excitation was kept constant, and absorbance of the samples at 337 nm was matched. By comparing the amount of triplet squaraine dye generated in each experiment, we were able to determine the triplet quantum yield (Φ_T) of C_{76} and C_{78} as 0.05 and 0.12, respectively. (Please note that these values of triplet quantum yield are relative to the triplet quantum yield of $C_{60} = 0.93$, a value obtained from the literature.[18]) It is interesting to note that the triplet quantum yield values for these two larger fullerenes are significantly smaller than that of C_{60} or C_{70}. A qualitative observation regarding the low triplet quantum yield has also been made earlier for larger fullerenes.[19,20] These results suggest that a nonradiative decay process is also dominant in the deactivation of the singlet excited states of larger fullerenes.

Pulse Radiolytic Generation of Excited Triplet States. Pulse radiolysis has been employed to generate and characterize excited triplet states of C_{60}, C_{70}, and several organic compounds in nonaqueous media such as toluene or benzene.[21−24] Radiolysis of a nitrogen-saturated toluene solution containing 0.02 M biphenyl yields long-lived excited triplets of biphenyl (^{3}BP). In the presence of fullerene we would expect intermolecular triplet−triplet energy transfer from the ^{3}BP* ($E_T = 64.5$ kcal/mol) to the lower lying triplets ($E_T = 35.34$ kcal/mol) of C_{76} and C_{78}. This route provides an elegant method for forming excited triplet states of the fullerenes bypassing the initial excited singlet state. The excited triplet state of biphenyl shows an absorption maximum around 360 nm.

In the present study, addition of various concentrations of C_{76} and C_{78} ($(0.2-2.5) \times 10^{-5}$ M) to the biphenyl solution resulted in the expected acceleration in the decay of the excited biphenyl (^{3}BP*) triplet. Parallel to the decay of ^{3}BP*, the formation of ($^3C_{76}$*) and ($^3C_{78}$*) was detected with maxima around 560 and 490 nm, respectively. The difference absorption spectrum for ($^3C_{76}$*) is shown in Figure 4B. The quenching rate constants of the energy transfer were determined from the decay kinetics of the transient absorption decay at 360 nm following pulse irradiation. In both cases, the quenching of the ^{3}BP* obeys eq 2, where k_{obs} is the observed first-order decay

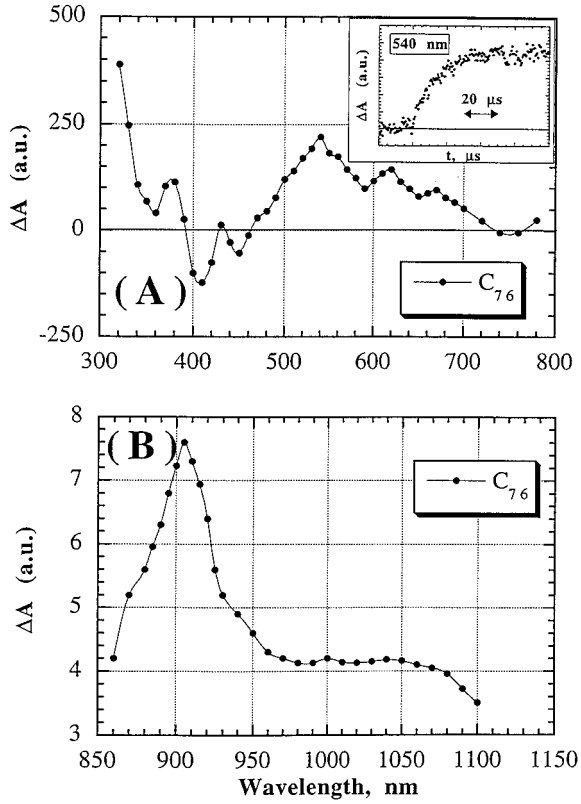

Figure 5. Transient absorption spectrum of C_{76}-radical anion obtained upon pulse radiolysis of 2.0×10^{-5} M C_{76} in a nitrogen-saturated toluene/2-propanol/acetone (8:1:1, v/v) mixture. (A) UV−vis and (B) NIR spectra of the radical anion of C_{76} are shown separately for the clarity of presentation.

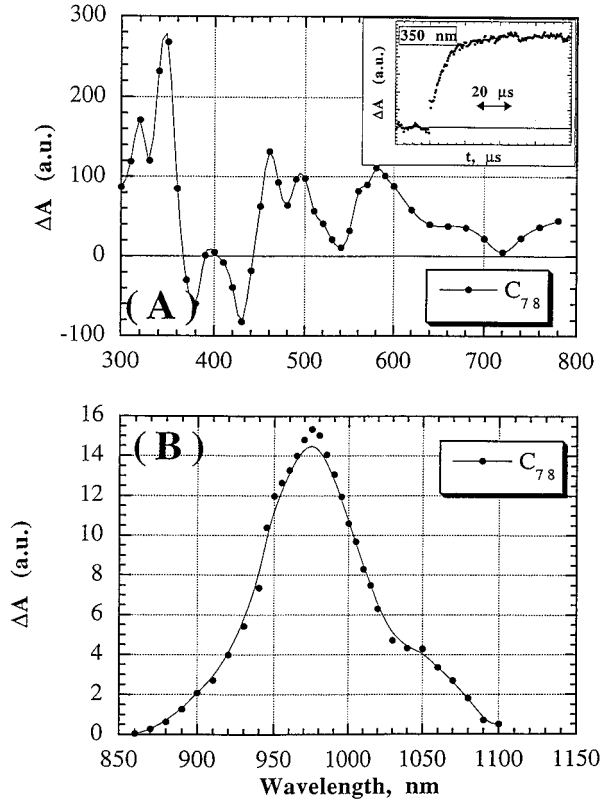

Figure 6. Transient absorption spectrum of fullerene-radical anion obtained upon pulse radiolysis of 2.0×10^{-5} M C_{78} in a nitrogen-saturated toluene/2-propanol/acetone (8:1:1, v/v) mixture. (A) UV−vis and (B) NIR spectra of the radical anion of C_{78} are shown separately.

rate constant, k_d is the intrinsic decay rate constant of ^{3}BP*, k_q is the bimolecular quenching rate constant, and (Q) is the concentration of fullerene.

$$k_{obs} = k_d + k_q(Q) \tag{2}$$

The observed first-order rate constants k_{obs} were linearly dependent on the fullerene concentration, as shown for C_{76} in Figure 4A. The intercepts agree well with the k_d value in the absence of a quencher representing the bimolecular quenching reaction,

$$^3\text{BP}^* + C_{76}\ (\text{or } C_{78}) \xrightarrow{k_q} \text{BP} + {}^3C_{76}\ (\text{or } {}^3C_{78}) \tag{3}$$

The T−T energy transfer rate constants are summarized in Table 2. The rate constants of 1.1×10^{10} M^{-1} s^{-1} for C_{76} and 1.3×10^{10} M^{-1} s^{-1} for C_{78} derived from the slopes of the linear plots of k_{obs} vs fullerene concentration are slightly lower than those obtained for C_{60} and C_{70}.[19,21] The excited triplet of fullerenes decayed via a dose-independent first-order kinetics, on a time scale of 100 μs, to regenerate the ground state (see inset in Figure 4B).

Radiolytic Reduction of C_{76} and C_{78}. One-electron reduction of fullerenes was achieved by reaction of these substrates with $(CH_3)_2{}^{\bullet}COH$ radicals generated in a toluene/2-propanol/acetone (8:1:1, v/v) solvent mixture. The reducing species generated in this solvent mixture is the radical formed by hydrogen abstraction from 2-propanol and from electron capture of acetone followed by subsequent protonation to form $(CH_3)_2{}^{\bullet}COH$ radicals.

$$(CH_3)_2CHOH \xrightarrow{e} e_{sol} + (CH_3)_2CH(OH)^{\bullet+} \tag{4}$$

$$(CH_3)_2CH(OH)^{\bullet+} \rightarrow (CH_3)_2{}^{\bullet}COH + H^+ \tag{5}$$

$$e_{sol} + (CH_3)_2CO \rightarrow (CH_3)_2{}^{\bullet}CO^- \tag{6}$$

$$(CH_3)_2{}^{\bullet}CO^- + H^+ \rightarrow (CH_3)_2{}^{\bullet}COH \tag{7}$$

The strongly reducing $(CH_3)_2{}^{\bullet}COH$ radicals ($E^{\circ}_{1/2} = -1.39$ V vs NHE) are then expected to undergo electron transfer with the fullerenes (reaction 8).[25]

$$(CH_3)_2{}^{\bullet}COH + C_{76}/C_{78} \rightarrow (CH_3)_2CO + (C_{76}{}^{\bullet-})/(C_{78}{}^{\bullet-}) + H^+ \tag{8}$$

The difference absorption spectra obtained upon electron pulse irradiation of C_{76} ($\sim 2 \times 10^{-5}$ M) and C_{78} ($\sim 4 \times 10^{-5}$ M) in a N_2-saturated, toluene/2-propanol/acetone mixture (8:1:1 v/v) are shown in Figures 5 (A,B) and 6 (A,B), respectively. The difference absorption spectra recorded in the visible and NIR region mostly show a positive change in the absorption, indicating thereby a higher extinction coefficient of the fullerene-radical anions than the corresponding extinction coefficient of the ground state itself. A bleaching is seen around 410 nm for (C_{76}) and in the wavelength range between 370 and 440 nm for C_{78}. This spectral region where bleaching is observed corresponds to the absorption peaks in the ground state spectra. Since the radiolysis experiments produce exclusively reductive species,[26,27] under the current experimental conditions the observed changes indicate one-electron reduction of C_{76} and C_{78}.

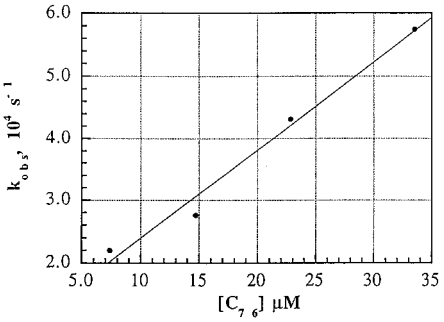

Figure 7. Dependence of k_{obs} on the concentration of C_{76}. The transient absorption monitored at 540 nm corresponded to the reduction of C_{76} by $(CH_3)_2$•C(OH) radical in a deoxygenated toluene/2-propanol/acetone (8:1:1, v/v) mixture.

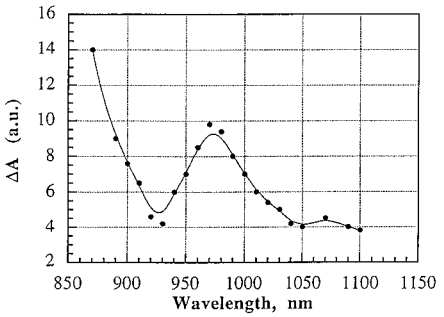

Figure 8. Difference absorption spectrum recorded immediately after a 500-ns electron pulse in an nitrogen-saturated solution of 2×10^{-5} M C_{78} in dichloromethane.

Reduced forms of fullerenes have been shown to possess characteristic absorption bands in the NIR range. For example, radical anions of C_{60} and C_{70} exhibit prominent absorption bands at 1080 and 880 nm, respectively. We also probed the spectral features of $C_{76}^{\bullet-}$ and $C_{78}^{\bullet-}$ in the infrared region (850−1150 nm). Distinct absorption bands of C_{76} at 910 nm (Figure 5B) and C_{78} at 975 nm (Figure 6B) were observed for both fullerenes. These spectral characteristics serve as fingerprints that would aid monitoring of the one-electron reduction process involving C_{76} and C_{78}.

Kinetic traces recorded at 540 nm (C_{76}) and 350 nm (C_{78}) are displayed in the insets of Figures 5A and 6A, respectively. The changes in absorption, which occur exponentially with average half-lives ($t_{1/2}$) of 10 and 6 μs, are attributed to the reduction of the fullerenes by $(CH_3)_2$•COH radicals (reaction 8). From the slopes of the plot of pseudo-first-order rate constant ($k_{obs} = \ln 2/t_{1/2}$) vs fullerene concentration (see for example, Figure 7) we obtained bimolecular rate constants of 1.3×10^9 and 1.6×10^9 M^{-1} s^{-1} for the reduction of C_{76} and C_{78}, respectively. The rate constants are summarized in Table 2. Comparison of these values has also been made with other fullerenes. The rate constants for the reduction of C_{76} and C_{78} are slightly higher than the value of 8.5×10^8 M^{-1} s^{-1} for the reduction of C_{60} and 8×10^8 M^{-1} s^{-1} for the reduction of C_{70} with $(CH_3)_2$•COH radicals. We attribute this difference to the lower reduction potential of larger fullerenes (Table 2).

Radical-induced reduction of these higher fullerenes was also studied in N_2-purged 2-propanol solution, as it leads to the formation of reducing species, e_{sol} and $(CH_3)_2$•COH radicals. Practically the same results were obtained in these experiments. In the present experiments reaction with the solvated electrons dominates the reduction of fullerenes (reaction 9):

$$e_{sol} + C_{76}\ (\text{or } C_{78}) \rightarrow C_{76}^{\bullet-}\ (\text{or } C_{78}^{\bullet-}) \qquad (9)$$

Since the solubility of fullerenes in alcohols and other polar solvents is extremely poor, the large and hydrophobic surface of the fullerene core led to the formation of aggregates with indefinite sizes in polar solvents. The lack of information regarding actual fullerene concentration makes the determination of meaningful kinetic analysis rather difficult.

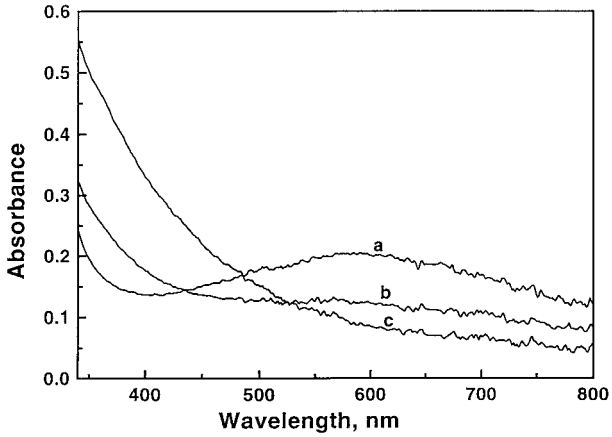

Figure 9. Absorption spectra of 10 mM TiO_2 colloidal in toluene/ethanol (1:1, v/v) recorded in a 2 mm pathlength cell (a) after UV illumination for 3 min. Spectra b and c were recorded after addition of C_{78} solution (5 and 15 μM, respectively) to the preirradiated TiO_2 suspension.

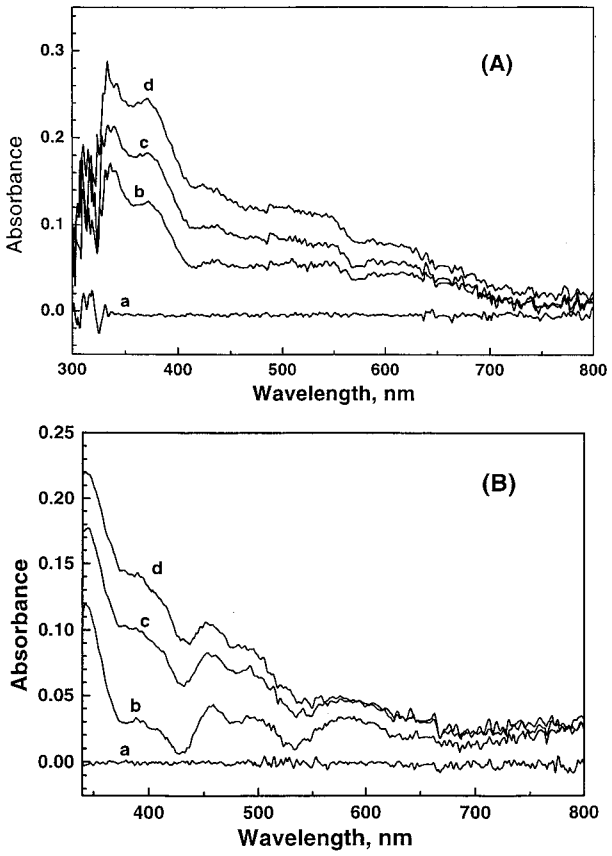

Figure 10. (A) Difference absorption spectrum of $C_{76}^{\bullet-}$. The spectra were recorded in a 2 mm pathlength cell following the UV irradiation of deaerated 10 mM colloidal TiO_2 in toluene/ethanol (1:1, v/v) containing C_{76}. The unirradiated (C_{76}/TiO_2) sample was used as a reference. (B) Difference absorption spectrum of $C_{78}^{\bullet-}$. The spectra were recorded in a 2 mm pathlength cell following the UV irradiation of deaerated 10 mM colloidal TiO_2 in toluene/ethanol (1:1, v/v) containing C_{78}. The unirradiated (C_{78}/TiO_2) sample was used as a reference.

Radiolytic Oxidation of C_{76} and C_{78}. Fullerenes are rather difficult to oxidize and usually undergo irreversible oxidation

with few selective oxidizing species. However, one-electron oxidation of fullerenes can be conveniently studied by irradiating a solution of this solute in dichloromethane (CH_2Cl_2). The radical cations $(CH_2Cl_2)^{\bullet+}$ generated via ionization of the solvent

$$CH_2Cl_2 \xrightarrow{e} e_{sol} + (CH_2Cl_2)^{\bullet+} \quad (10)$$

are strong oxidizing species that remove an electron from fullerenes, as shown in previous studies on C_{60}.[26] The lower oxidation potential of C_{76} and C_{78} relative to C_{60} and C_{70} should facilitate their oxidation as a result of the following reaction.

$$C_{76}\ (\text{or } C_{78}) + (CH_2Cl_2)^{\bullet+} \rightarrow C_{76}^{\bullet+}\ (\text{or } C_{78}^{\bullet+}) + CH_2Cl_2 \quad (11)$$

Absorption changes recorded upon radical-induced oxidation of C_{76} (2×10^{-5} M) in deoxygenated CH_2Cl_2 exhibited a distinct maximum at 960 nm accompanied by a shoulder located around 1050 nm. In analogy to C_{60} and C_{70}, these changes can be attributed to the formation of the fullerene-radical cation. Corresponding NIR features for $C_{78}^{\bullet+}$ were much weaker, showing a band around 980 nm (Figure 8). The observed absorption features constitute characteristic absorption bands in the infrared region. The spectral assignment in the near IR has been further substantiated by synthesizing a cation salt ($(C_{76})^{\bullet+}(CB_{11}H_6Br_6^-)$ (hexabromo carborane).[28] A prominent absorption band at 780 nm was reported in this work.

The buildup of the radical cation absorption could not be further time-resolved. From the absorption−time trace it is apparent though that the oxidation process is completed within 1 μs. Accordingly, we expect a lower limit of 2×10^{10} M^{-1} s^{-1} as a rate constant for the radical-induced oxidation of C_{76} and C_{78}.

It should be noted that the one-electron-oxidation products of C_{76} and C_{78} were short-lived and decayed within a few microseconds. We expect the decay of $C_{76}^{\bullet+}$ proceeds via the same mechanism as observed with $C_{60}^{\bullet+}$, i.e., formation of a dimer radical cation (reaction 12).

$$C_{76}^{\bullet+}\ (\text{or } C_{78}^{\bullet+}) + C_{76}\ (\text{or } C_{78}) \rightarrow (C_{76})_2^{\bullet+}\ (\text{or } (C_{78})_2^{\bullet+}) \quad (12)$$

By analyzing the decay as a pseudo-first-order process, we obtain $t_{1/2} = 20$ μs (5.9×10^{-6} M) and $t_{1/2} = 14$ μs (2.9×10^{-6} M), respectively. The bimolecular rate constants were 7.9×10^8 and 9.8×10^8 M^{-1} s^{-1} for C_{76} and C_{78}, respectively. These rate constants are smaller compared to those of C_{60} (6×10^9 M^{-1} s^{-1})[26] and C_{70} (6.0×10^9 M^{-1} s^{-1}).[29]

Reduction of C_{76} and C_{78} in Colloidal TiO_2 Suspension. A photoelectrochemical approach for reducing fullerenes is a convenient way to carry out one-electron reduction of fullerenes. For example, the use of TiO_2 and ZnO semiconductor nanoclusters to carry out controlled one-electron reduction of C_{60} and C_{70} under UV excitation has been demonstrated by us and others.[27,30]

The semiconductor TiO_2 is an excellent choice to carry out one-electron reduction of C_{76} and C_{78} since the energy of its conduction bands ($E_{CB} = -0.5$ V vs NHE at pH 7) thermodynamically favors one-electron reduction of fullerenes ($E^\circ_{red} > -0.1$ V vs NHE).[31]

$$TiO_2 + h\nu \rightarrow TiO_2\ (h + e) \rightarrow TiO_2\ (h_t + e_t) \quad (13)$$

$$TiO_2\ (e_t) + C_{76}\ (\text{or } C_{78}) \rightarrow TiO_2 + C_{76}^{\bullet-}\ (\text{or } C_{78}^{\bullet-}) \quad (14)$$

Two different sets of experiments were carried out to characterize the anion radical of C_{76} and C_{78}. In the first set we avoided direct photolysis of fullerenes by reacting them with preirradiated TiO_2 suspensions. A deaerated suspension of colloidal TiO_2 (10 mM) in toluene/ethanol (1:1, v/v) was first irradiated with a 1000-W xenon/mercury lamp to induce charge separation followed by trapping of holes (h_t) and electrons (e_t) within the semiconductor colloids (reaction 13). The solution turned blue as the UV irradiation was continued for 3−5 min (spectrum a in Figure 9). This blue coloration of the colloidal suspension is a characteristic feature of trapped electrons in TiO_2 colloids.[31−34] A known amount of deaerated C_{76} (or C_{78}) solution (100 μM) in toluene was successively added to both sample and reference cells (total volume 1 mL). A cell containing toluene/ethanol (1:1, v/v) was used as the reference. The spectrum recorded after the addition of C_{78} (spectrum b and c in Figure 9) shows a decreased absorption of the broad absorption band at 700 nm and an increased absorption at wavelengths below 450 nm. The decrease in the absorption at 700 nm indicates that the trapped electrons are scavenged by fullerenes to produce $C_{76}^{\bullet-}$ (reaction 14). It should be noted that the trapped electrons in a preirradiated TiO_2 suspension are relatively long-lived and do not decay when stored under N_2 atmosphere.

In the second set of experiments we photolyzed the samples containing TiO_2 and fullerene in toluene/ethanol (1:1, v/v) medium. The spectral features of $C_{76}^{\bullet-}$ and $C_{78}^{\bullet-}$ were further probed by subtracting the contribution of TiO_2 absorption to the overall spectrum. The difference absorption spectra recorded following photolysis show increased absorption at 330 nm with increasing photolysis time (Figure 10 A,B). The absorption bands observed at 350−650 nm are similar to the spectral features of radical anions of C_{76} and C_{78}, as discussed earlier in radiolytic reduction reactions. The stability of fullerene anion radicals in N_2 atmosphere has thus enabled us to characterize them with conventional spectrophotometry.

Acknowledgment. The work described herein was supported by the Office of Basic Energy Sciences of the U.S. Department of Energy. This is Contribution No. NDRL-3994 from the Notre Dame Radiation Laboratory.

References and Notes

(1) Bendale, R. D.; Zerner, M. C. *J. Phys. Chem.* **1995**, *99*, 13830.

(2) Kikuchi, K.; Nakahara, N.; Honda, M.; Suzuki, S.; Katada, M.; Shiromaru, H.; Yamauchi, K.; Ikemoto, I.; Kuramochi, T.; Hino, S.; Achiba, Y. *Chem. Lett* **1991**, 1607.

(3) Kikuchi, K.; Nakahara, N.; Wakabayashi, T.; Suzuki, S.; Shiromaru, H.; Miyake, Y.; Sato, Y.; Ikemoto, I.; Kainosho, M.; Achiba, Y. *Nature* **1992**, *357*, 142.

(4) Achiba, Y.; Kikuchi, K.; Muccini, M.; Orlandi, G.; Ruani, G.; Taliani, C.; Zamboni, R.; Zerbetto, F. *J. Phys. Chem.* **1994**, *98*, 7933.

(5) Selegue, J. P.; Shaw, J. P.; Guarr, T. F.; Meier, M. S. In *Recent Advances in the Chemistry and Physics of Fullerenes and Related Materials*.; Kadsish, K. M., Ruoff, R. S., Eds.; The Electrochemical Society, Inc.: Pennington, NJ, 1994; Vols. 94−24, p 1274.

(6) Benz, M.; Fanti, M.; Fowler, P. W.; Fuchs, D.; Kappes, M. M.; Lehner, C.; Michel, R. H.; Orlandi, G.; Zerbetto, F. *J. Phys. Chem.* **1996**, *100*, 13399.

(7) Armbruster, J. F.; Romberg, H. A.; Schweiss, P.; Adelmann, P.; Knupfer, M.; Fink, J.; Michel, R. H.; Rockenberger, J.; Hennrich, F.; Schreiber, H.; Kappes, M. M. *Z. Phys. B* **1994**, *95*, 469.

(8) Michel, R. H.; Schreiber, H.; Gierden, R.; Hennrich, F.; Rockenberger, J.; Beck, R. D.; Kappes, M. M.; Lehner, C.; Adelmann, P.; Armbruster, J. F. *Ber. Bunsen-Ges. Phys. Chem.* **1994**, *98*, 975.

(9) Orlandi, G.; Zerbetto, F.; Fowler, P. W.; Manolopoulos, D. E. *Chem. Phys. Lett.* **1993**, *208*, 441.

(10) Sauve, G.; Kamat, P. V. In *Recent Advances in the Chemistry and Physics of Fullerenes and Related Materials*; Kadish, K. M., Ruoff, R. S., Eds.; The Electrochemical Society, Inc.: Pennington, NJ, 1995; Vols. 95−10, p 399.

(11) Kamat, P. V.; Sauve, G.; Guldi, D. M.; Asmus, K.-D. *Res. Chem. Intermed.* **1997**, *23*, 575.

(12) Yang, Y.; Arias, F.; Echegoyen, L.; Felipe Chibante, L. P.; Flanagan, S.; Robertson, A.; Wilson, L. J. *J. Am. Chem. Soc.* **1995**, *117*, 7801.

(13) Ruoff, R. S.; Kadish, K. M.; Boulas, P.; Chen, E. C. M. *J. Phys. Chem.* **1995**, *99*, 8843.

(14) Kikuchi, K.; Nakahara, N.; Wakabayashi, T.; Honda, M.; Matsumiya, H.; Moriwaki, T.; Suzuki, S.; Shiromaru, H.; Sato, Y.; Yamauchi, K.; Ikemoto, I.; Achiba, Y. *Chem. Phys. Lett.* **1992**, *88*, 177.

(15) Zeng, Y.; Biczok, L.; Linschitz, H. *J. Phys. Chem.* **1992**, *96*, 5237.

(16) Foote, C. S. *Top. Curr. Chem.* **1994**, *169*, 347.

(17) Sauve, G.; Kamat, P. V.; Thomas, K. G.; Thomas, J.; Das, S.; George, M. V. *J. Phys. Chem.* **1996**, *100*, 2117.

(18) Biczok, L.; Linschitz, H.; Walter, R. I. *Chem. Phys. Lett.* **1992**, *195*, 339.

(19) Sauve, G.; Kamat, P. V.; Ruoff, R. S. *J. Phys. Chem.* **1995**, *99*, 2162.

(20) Terazima, M.; Hirota, N.; Shinohara, H.; Asato, K. In *Fullerenes*; Ruoff, R., Kadish, K., Eds.; The Electrochemical Society: Pennington, NJ, 1995; Vols. 95−10, p 267.

(21) Dimitrijevic, N. M.; Kamat, P. V. *J. Phys. Chem.* **1992**, *96*, 4811.

(22) Bensasson, R. V.; Hill, T. J.; Lambert, C.; Land, E. J.; Leach, S.; Truscott, T. G. *Chem. Phys. Lett.* **1993**, *201*, 326.

(23) Priyadarsini, K. I.; Mohan, H.; Birkett, P. R.; Mittal, J. P. *J. Phys. Chem.* **1996**, *100*, 501.

(24) Guldi, D. M.; Hungerbühler, H.; Asmus, K. D. *J. Phys. Chem.* **1995**, *99*, 9380.

(25) Wardman, P. *Phys. Chem. Ref. Data* **1989**, *18*, 1637.

(26) Guldi, D. M.; Hungerbühler, H.; Janata, E.; Asmus, K. D. *J. Phys. Chem.* **1993**, *97*, 11258.

(27) Stasko, A.; Brezova, V.; Biskupic, S.; Dinse, K.-P.; Schweitzer, P.; Baumgarten, M. *J. Phys. Chem.* **1995**, *99*, 8782.

(28) Bolskar, R. D.; Mathur, R. S.; Reed, C. A. *J. Am. Chem. Soc.* **1996**, *118*, 13093.

(29) Guldi, D. M.; Hungerbühler; Wilhelm, M.; Asmus, K.-D. *J. Chem. Soc., Faraday Trans.* **1994**, *90*, 1391.

(30) Kamat, P. V. *J. Am. Chem. Soc.* **1991**, *113*, 9705.

(31) Kamat, P. V.; Bedja, I.; Hotchandani, S. *J. Phys. Chem.* **1994**, *98*, 9137.

(32) Bahnemann, D.; Henglein, A.; Lilie, J.; Spanhel, L. *J. Phys. Chem.* **1984**, *88*, 709.

(33) Serpone, N.; Lawless, D.; Khairutdinov, R.; Pelizzetti, E. *J. Phys. Chem.* **1995**, *99*, 16655.

(34) Colombo, D. P. J.; Rousal, K. A.; Saeh, J.; Skinner, D. E.; Bowman, R. M. *Chem. Phys. Lett*. **1995**, *232*, 207.

(35) Ebbesen, T. W.; Tanigaki, K.; Kuroshima, S. *Chem. Phys. Lett.* **1991**, *181*, 501.

(36) Arbogast, J. W.; Foote, C. S. *J. Am. Chem. Soc*. **1991**, *113*, 8886.

(37) Tanigaki, K.; Ebbesen, T. W.; Kuroshima, S. *Chem. Phys. Lett.* **1991**, *185*, 189.